Harmonic and reactive behavior of the quasiparticle tunnel current in SIS junctions

Harmonic and reactive behavior of the quasiparticle tunnel current in SIS junctions

H. Rashid,[a] V. Desmaris, A. Pavolotsky, and V. Belitsky
Group for Advanced Receiver Development, Earth and Space Sciences Department, Chalmers University of Technology, Gothenburg, 412 96, Sweden

(Received 7 January 2016; accepted 7 April 2016; published online 19 April 2016)

In this paper, we show theoretically and experimentally that the reactive quasiparticle tunnel current of the superconductor tunnel junction could be directly measured at specific bias voltages for the higher harmonics of the quasiparticle tunnel current. We used the theory of quasiparticle tunneling to study the higher harmonics of the quasiparticle tunnel current in superconducting tunnel junction in the presence of rf irradiation. The impact of the reactive current on the harmonic behavior of the quasiparticle tunnel current was carefully studied by implementing a practical model with four parameters to model the dc I-V characteristics of the superconducting tunnel junction. The measured reactive current at the specific bias voltage is in good agreement with our theoretically calculated reactive current through the Kramers-Kronig transform. This study also shows that there is an excellent correspondence between the behavior of the predicted higher harmonics using the previously established theory of quasiparticle tunnel current in superconducting tunnel junctions by J.R. Tucker and M.J. Feldman and the measurements presented in this paper.
[http://dx.doi.org/10.1063/1.4947133]

I. INTRODUCTION

The superconductor-insulator-superconductor (SIS) junctions carry two types of tunnel currents, namely the Cooper-pair tunnel current described by B.D. Josephson[1,2] and the quasiparticle tunnel current[3–5] (QTC). In the presence of rf radiation with sufficient quanta size, the tunnel current consists of both a dissipative and a reactive component. Unlike the QTC, the Cooper-pair tunnel currents have been studied extensively.[1,4] The dissipative QTC determines the dc I-V characteristics, whereas the reactive part of the QTC is calculated through the Kramers-Kronig transformation of the dissipative part of QTC. Furthermore, there is no obvious way to directly measure the reactive QTC as it is the imaginary part of the total QTC. Instead, the reactive part of the QTC has so far only been studied indirectly by comparing theoretical and measured values of the quantum susceptance.[6,7]

Until now, little work has been done in exploring higher order QTC harmonics in SIS junctions.[8,9] Recently, an experimental paper published by Billade et al.,[10] experimentally proved the presence of the second harmonic generated by an SIS tunnel junction series array consisting of 68 elements. However, the experimental results were not supported by any physical modelling and the importance of the reactive current was overlooked.

In 1985 J.R Tucker and M.J Feldman published a paper concerning the physics of the QTC in SIS junctions and its applications for quantum detection at millimeter wavelengths.[5] The derivation of the closed form expression for the QTC in the SIS junction shows that there are higher order QTC harmonics.[5] The behavior of the higher harmonics of the QTC in SIS junctions would be especially interesting, since the quasiparticle tunneling current voltage (I-V) characteristic of the

[a]Corresponding author. Email: hawal@chalmers.se

junction exhibits extremely sharp quasi-particle nonlinearity. Consequently, the higher order QTC harmonics in an ideal SIS junction (where the quasiparticle nonlinearity is infinitely sharp) would be similar to the Fourier series of a Dirac delta function. Consequently, one possible application might be that the SIS junction could be used as a current source with very pure signal.

In this paper, we study the reactive part of the QTC and its impact on the QTC harmonic behavior. Furthermore, we demonstrate that direct measurement of the reactive QTC can be carried out at specific bias voltages for the higher harmonics of the QTC. In this study, we first study the behavior of the QTC harmonics and then the impact of the reactive current on the harmonic behavior of the QTC. Furthermore, we analyze the influence of the SIS junction parameters such as normal state resistance and the transition width at gap voltage on the reactive QTC.

II. THEORY

The calculations in this paper consider only the higher harmonics of the QTC in the SIS junctions induced by a single frequency rf signal. We consider the case when the Josephson effect is suppressed with an external magnetic field. The derivation of QTC equations is shown in great detail by J.R Tucker and M.J Feldman.[5]

The time averaged QTC in an SIS junction may be written in as[4,5]

$$< I(t) >= Im \int_{-\infty}^{\infty}\int_{-\infty}^{\infty} d\omega' d\omega'' W(\omega') W^*(\omega'') \times e^{-i(\omega'-\omega'')t} j\left(V_0 + \frac{\hbar\omega'}{e}\right) \tag{1}$$

where $W(\omega')$ is the Fourier transform of the phase factor, V_0 is the dc bias voltage, and $j(V)$ is the complex physical response current of the tunnel junction. The complex response current of the tunnel junction is written as follow:

$$j(V) = iI_{dc}(V) + I_{KK}(V) \tag{2}$$

I_{KK} is the reactive part of the tunnel current, which relates to the dissipative part through the Kramers-Kronig transform:

$$I_{KK}(V) = P\int_{-\infty}^{\infty} \frac{d\bar{V}}{\pi} \frac{I_{dc}(\bar{V}) - \bar{V}/R_N}{\bar{V} - V} \tag{3}$$

where R_N is the normal state resistance of the junction and P is the Cauchy principal value. In the presence of rf radiation with a purely sinusoidal ac voltage, $V(t)$, across the tunnel barrier, equation (1) turns into[5]:

$$< I(t) >= a_0 + \sum_{m=1}^{\infty} J_m(\alpha)(a_m \cos(m\omega t) + b_m \sin(m\omega t) \tag{4}$$

where $J_m(\alpha)$ is the Bessel function of the first kind, m is the harmonic number and α is the amplitude of the applied ac voltage, V_{ac}, normalized with its photon energy, henceforward referred to as the pumping factor:

$$\alpha = \frac{e}{\hbar\omega_{ac}} V_{ac} \tag{5}$$

It is now clear that the time averaged current induced by the ac voltage, $V(t)$ contains all harmonic frequencies with amplitudes given by:

$$\begin{aligned} 2a_m &= \sum_{n=-\infty}^{\infty} J_n(\alpha)(J_{n+m}(\alpha) + J_{n-m}(\alpha)) I_{dc}\left(V_{bias} + \frac{n\hbar\omega}{e}\right) \\ 2b_m &= \sum_{n=-\infty}^{\infty} J_n(\alpha)(J_{n+m}(\alpha) - J_{n-m}(\alpha)) I_{KK}\left(V_{bias} + \frac{n\hbar\omega}{e}\right) \end{aligned} \tag{6}$$

where $a_0\,(m=0)$ is the pumped dc QTC.

The Fourier transform of equation (4) allows us to study the induced current in the frequency domain for each harmonic:

$$\hat{I}(V_0,\omega) = \pi a_0 + 2\pi \sum_{m=1}^{\infty} [a_m - ib_m]\,\delta(\omega - m\Omega) = \pi a_0 + I_{RF} \tag{7}$$

where

$$I_{RF} = I' - iI'' \tag{8}$$

and

$$\begin{aligned} I' &= \pi \sum_{m=1}^{\infty} \sum_{n=-\infty}^{\infty} J_n(\alpha)\,(J_{n+m}(\alpha) + J_{n-m}(\alpha))\, I_{dc}\left(V_{bias} + \frac{n\hbar\omega}{e}\right) \\ I'' &= \pi \sum_{m=1}^{\infty} \sum_{n=-\infty}^{\infty} J_n(\alpha)\,(J_{n+m}(\alpha) - J_{n-m}(\alpha))\, I_{KK}\left(V_{bias} + \frac{n\hbar\omega}{e}\right) \end{aligned} \tag{9}$$

Even though it seems controversial, but indeed the real part of the induced current depends on the imaginary part of the current response function; and in turn, the imaginary part of the induced current depends on the real part of the current response function. As can be seen from the equation (8), the real part of the induced current is proportional to I_{dc}, which is the imaginary part of the current response function. Likewise, the imaginary part of the induced current is proportional to I_{KK}, which is the real part of the current response function.

The behavior of the real part of the response functions is of particular interest, as it determines the maximum value of the induced QTC. For example the real part of the current response function of an ideal SIS junction ($\alpha = 0$) at zero Kelvin would be divergent at the gap voltage V_g due to the extremely sharp current onset in the imaginary part of the current response function. The gap voltage of the SIS junction is defined as:

$$V_g = \frac{2\Delta}{e} \tag{10}$$

where Δ is the gap energy of the superconductor, i.e., an energy of 2Δ is required to break a Cooper pair into two quasiparticles. However, in any practical SIS junction, the transition width at gap voltage has a certain finite width due to the non-zero operation temperature and other factors limiting junction quality, e.g., purity of the superconductors constituting the SIS junctions. Correspondingly, the maximum value of the real part of the response current, I_{KK} would depend on the SIS junction quality.

A. Modelling of DC I-V characteristics

The real and imaginary part of the response function in equation (2) must be obtained in order to compute the closed form expression of the quasiparticle tunnel current given by (8)-(9). The imaginary part of the current response function could be found either through the measured dc I-V characteristics or from complex theoretical expressions, which has to be computed numerically.[4,5] The real part of the current response function, i.e., I_{KK} could be obtained through equation (3). In this paper we use an empirical model, equation (11) for the imaginary part of the junction's current response function to study I_{KK} current effect on the overall QTC.

$$\begin{aligned} I_{dc}(V) = &\left[\frac{V}{R_L}\left(\frac{1}{1+e^{-a(V+V_g)}}\right) + \frac{V}{R_N}\left(\frac{1}{1+e^{a(V+V_g)}}\right)\right] \\ &+ \left[\frac{V}{R_L}\left(\frac{1}{1+e^{a(V-V_g)}}\right) + \frac{V}{R_N}\left(\frac{1}{1+e^{-a(V-V_g)}}\right)\right] \end{aligned} \tag{11}$$

The empirical model that we suggest has four fitting parameters: R_L is the subgap resistance, R_N is the normal resistance, V_g is the gap voltage, and the coefficient, a, accounts for the transition width at gap voltage, henceforward referred to as a current onset sharpness. Three out of the four fitting

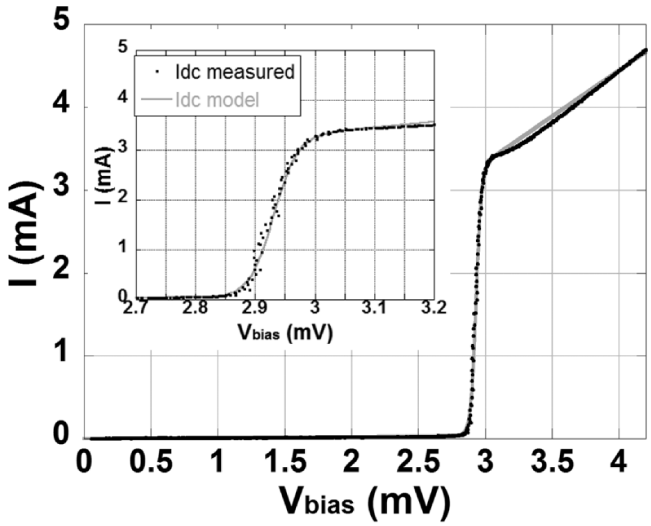

FIG. 1. Modelled I-V according to equation (13) compared with measured I-V. The inset shows the I-V near the gap voltage. The solid gray line corresponds to the modelled I-V, whereas the dotted plot corresponds to the measured I-V.

parameters (R_L, R_N, and V_g) used in the empirical model are physical parameters, which are extracted from measured I-V characteristics.[11] The current onset sharpness coefficient, a, is estimated through fitting, which has a typical value of approximately $3 - 4 \cdot 10^4$ (V^{-1}) for the Nb-AlOx-Nb junctions produced in-house.[12] This parameter can be used as a measure of junction quality, as presented further in the next section.

The first square bracket term in the equation (11) is the dc quasiparticle tunnel current with respect to negative bias voltage, whereas the second square bracket term accounts for positive bias voltage. The two terms inside the square brackets refer to the subgap and normal electron current i.e., the current before and after the gap onset, whereas the Fermi-Dirac-like functions define where the onset occurs and its sharpness. Figure 1 shows the comparison between the modelled and the measured I-V characteristics. As can clearly be seen, the modelled I-V characteristic of the SIS junction is in a very good agreement with the measured one.

B. The influence of I_{KK} on the higher harmonics of the quasiparticle tunnel current

It can be seen from equation (8) and (9) that the imaginary part of the induced current is proportional to the real part of the current response function I_{KK}. Furthermore, the relationship between the QTC onset sharpness, i.e., the fitting parameter, a, and a relative maximum/minimum value could be shown by taking the second partial derivative of the I_{KK}.

$$\frac{d^2 I_{KK}(V)}{dV^2} = \frac{1}{R_L}\left[\frac{1}{(V-V_g)\left(1+e^{a(V-V_g)}\right)} - \frac{V}{(V-V_g)^2\left(1+e^{a(V-V_g)}\right)} - \frac{Vae^{a(V-V_g)}}{(V-V_g)\left(1+e^{a(V-V_g)}\right)^2}\right]$$
$$+\frac{1}{R_N}\left[\frac{1}{(V-V_g)\left(1+e^{-a(V-V_g)}\right)} - \frac{V}{(V-V_g)^2\left(1+e^{-a(V-V_g)}\right)} + \frac{Vae^{-a(V-V_g)}}{(V-V_g)\left(1+e^{-a(V-V_g)}\right)^2}\right] - \quad (12)$$
$$\frac{1}{R_N}\left[\frac{1}{V-V_g} - \frac{V}{(V-V_g)^2}\right]$$

For $V>0$ and in vicinity of V_g, one can estimate the second derivative to study the influence of current onset sharpness, normal resistance and subgap resistance for the case of non-ideal junction ($a \approx 1 \cdot 10^3 - 1 \cdot 10^5$):

$$\frac{d^2 I_{KK}(V)}{dV^2} \approx \frac{1}{R_L}\left[\frac{V_g a e^{-a\varepsilon}}{\varepsilon(1+e^{-a\varepsilon})^2} - \frac{V_g}{\varepsilon^2(1+e^{-a\varepsilon})}\right] - \frac{1}{R_N}\frac{V_g a e^{a\varepsilon}}{\varepsilon(1+e^{a\varepsilon})^2} \quad (13)$$

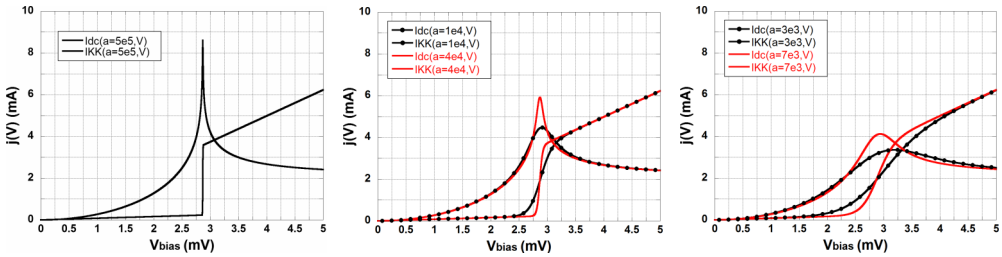

FIG. 2. The I_{KK} current with respect to the junction quality factor, a, which is associated with the onset sharpness. The values of the fitting parameter from left to right are a=5·10^5, 1·10^4, 4·10^4, 7·10^3 and 3·10^3. The sharper the onset current is the greater the maximum value of I_{KK}.

where $\varepsilon = V - V_g$; $\varepsilon \ll V_g$. Equation (13) shows that the peak value of the I_{KK} is not only dependent on the onset sharpness of the SIS junction but also on the normal (R_N) and the subgap (R_L) resistances.

From equation (13), it also follows that the higher junction quality factor, a (smaller transition width at gap voltage), the greater maximum/minimum peak value of I_{KK} current, which becomes divergent for ideal SIS junction ($a \to \infty$). Equation (3) was used to compute the I_{KK} current for different junction quality factors a, as shown in figure 2.

C. Quasiparticle tunnel current at higher harmonics

The discussion in the previous section treats the dc current response function, i.e. when α =0. The discussion is also valid when ac voltage applied across the SIS junction ($\alpha > 0$). In this case, there are non-linearities (steps) of current observed, which are separated by a photon voltage $n\hbar\omega/e$ due to the multiphoton process[3,5] that occurs. These characteristics are captured by equation (7).

The magnitudes of the real, imaginary, resultant and the dc part of the quasiparticle tunnel current with respect to the pumping factor, α, and bias voltage, V_{bias}, are shown in figure 3 for the 2nd, 3rd and 4th harmonics. Table I summarizes the SIS junction parameters used for calculations. The frequency of the applied ac voltage in this example is 100 GHz and the higher harmonics corresponds to 200, 300 and 400 GHz. The plots are normalized to the maximum value of the total current i.e., max ($|I_{RF}|$) in order to make the plots more clear. The maximum values of the current modulus are presented in each plot panel. Figure 3 shows that the peak values of the induced higher harmonics of the QTC are strongly dependent on the maximum value of the I_{KK} current. Also, as follows from the discussion in the Section II B above, in order to maximize the reactive current, thereby maximizing the modulus of the induced higher harmonics of the QTC in equation (8) the normal resistance should be low, whereas the subgap resistance and the onset sharpness coefficient, a, should be as high as possible for practical SIS junctions. This fact emphasizes upon the importance of the SIS junction quality quantified by parameter a.

D. Measuring the I_{KK} current

The real part of the current response function is found by the Kramers-Kronig transformation of the I_{dc} and is given by equation (3). Furthermore, there is no obvious way to directly measure this quantity as it is the imaginary part of the total QTC. Instead, the reactive part of the QTC has so far only been studied indirectly by comparing theoretical and measured values of the quantum

TABLE I. Coefficient values for the empirical IVC model of Nb-AlOx-Nb SIS junction.

Subgap resistance, R_L (Ω)	Normal resistance, R_N (Ω)	Gap voltage, Vg (mV) at 4 K	Onset coefficient, a (1/V)
55	0.91	2.92	4·10^4

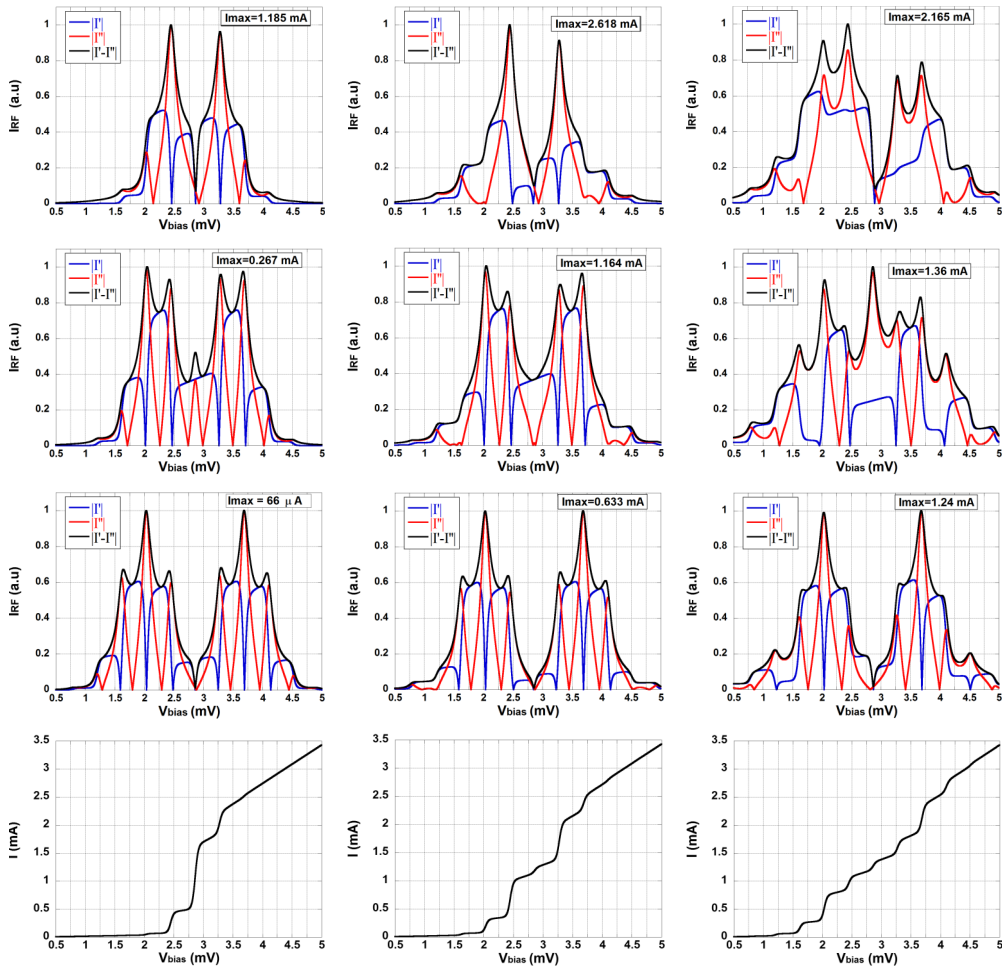

FIG. 3. Computation results following equation (7) for the applied ac voltage with the frequency of 100 GHz. The top three rows illustrate the magnitude of the real (dashed curve) ,imaginary (gray curve) parts ($|I'|$ and $|I''|$) and the resultant (dotted curve) i.e., $|I' - iI''|$ of the ac quasiparticle tunnel current whereas the fourth row illustrates the I-V characteristics with respect to the different pumping factors, α. The rows from first to third represent the results for the 2nd, 3rd and 4th harmonics correspondingly; the last row shows the p I-V characteristics of the SIS junctions; the columns from left to right represent the results for the $\alpha = 1$, 2 and 3 correspondingly.

susceptance.[6,7] The total measured induced QTC given by equation (8) and (9) consists of both the real and imaginary part. However, it can be shown that the real part of the induced QTC is zero for the higher harmonics at specific bias voltages and pumping factors $\alpha \leq 2$, and therefore, only the reactive part is present (see figure 3 and 4), which is proportional to I_{KK}. Furthermore, the maximum values of the induced QTC are found at these bias voltages and the pumping factor, α. This suggests that the real part of the current response function can be measured directly at the QTC harmonics. The voltage range in which the reactive part of the tunnel current can be measured this way is relatively narrow when the frequency of the applied ac voltage over the SIS junction is below 150 GHz. The voltage range could be somewhat increased by tuning the pumping factor, α. On the other hand, the voltage range is substantially increased for frequencies above 250 GHz (for specific values of α), see figure 4. This is due to the increase of the quanta size of the multi-photon process, as follows from the equation (9).

The extraction of the measured reactive QTC peak value is attainted by comparing the theoretical current modulus given by equation (8) and the measured current modulus. However, in order to calculate the theoretical current modulus, the pumping factor, α has to be known. This can be extracted by comparing the modeled and measured pumped dc I-V characteristics. The pumping

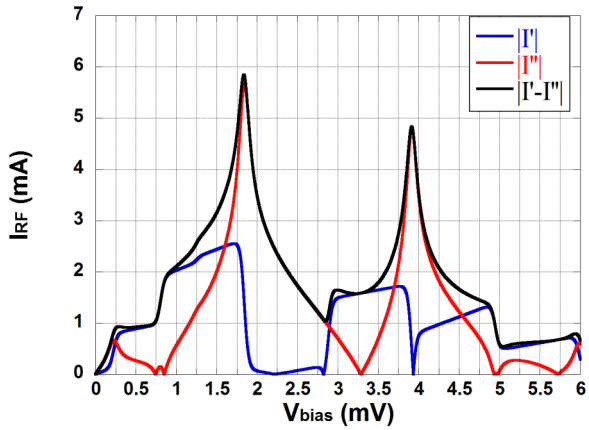

FIG. 4. Computation results for the second harmonic of the quasiparticle tunnel current following equation (7) for the applied ac voltage with the frequency of 250 GHz. The plot illustrate the magnitude of the real (dashed black curve), imaginary (solid gray curve) parts ($|I'|$ and $|I''|$) and the resultant (dotted black plot) i.e., $|I' - iI''|$ of the induced quasiparticle tunnel current at a pumping factor $\alpha = 2$.

factor in the model is adjusted until satisfactory agreement between model and measurement is achieved, see figure 6. Once the pumping factor is known, equation (11) and (3) are used to calculate the reactive current with respect to voltage, where the peak value of the calculated reactive current through equation (3) corresponds to the measured peak value without the Bessel function weighting at $I_{KK}\left(V_g - \hbar\omega/e\right)$. This extraction technique enables both direct measurement of the induced reactive QTC, which includes Bessel functions of the first kind and the real part of current response function, i.e., I_{KK} at the specific pumping values, and bias voltages.

III. EXPERIMENT AND RESULTS

In this paper, only the second harmonic of the QTC has been experimentally studied. The characterization of the SIS junction was carried out at 4 K with an experimental setup allowing accurate detection and measurements of the generated second harmonic of the QTC. Furthermore, the Josephson effect was suppressed by applying an external magnetic field. The measurement setup schematically shown in figure 5 consisted of a 4 K cryostat, an rf current source in order to apply a ac voltage across the SIS junction, a frequency down converter, a biasing circuit, waveguides and a spectrum analyzer. The output signal from the SIS junction is connected to a frequency down converter, where the output power of the down converted signal is measured with a spectrum analyzer. Furthermore, a low pass and bandpass filter was used at the input and output of the SIS junction respectively in order to ensure the proper propagation of the harmonic current and that only

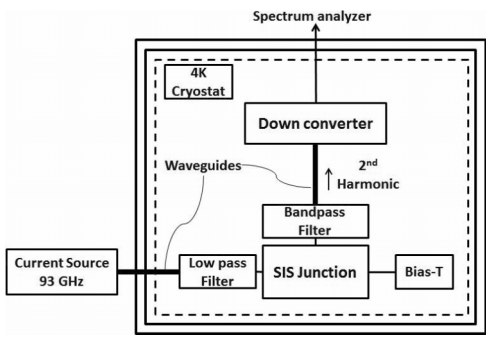

FIG. 5. Schematic of the experimental setup used to study the SIS junction. The SIS junction is investigated by measuring the power of the down converted output with a spectrum analyzer.

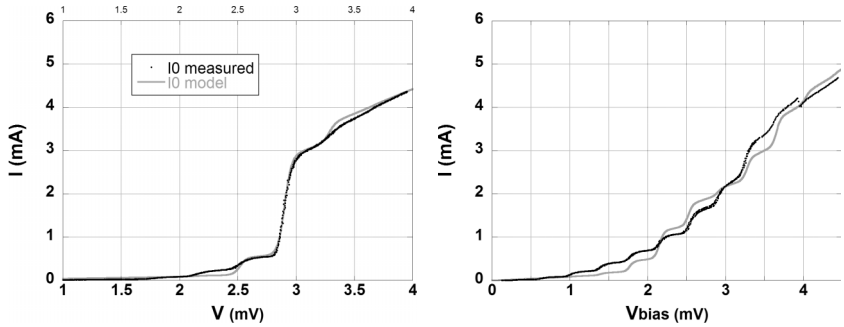

(a) (b)

FIG. 6. The static QTC of the pumped junction is compared with the model. The pumping factor in the model is adjusted until satisfactory agreement between model and measurement is achieved. Figure 6(a) The pumping factor $\boldsymbol{\alpha \approx 085}$. Figure 6(b) The pumping factor $\boldsymbol{\alpha \approx 3}$.

the second harmonic of the QTC is fed to the down converter. The frequency down converter, which operates at 163-211 GHz, consists of a dedicated SIS mixer similar to Ref. 13.

IV. RESULTS AND DISCUSSION

The physical parameters of the SIS (Nb-AlOx-Nb) junction such as gap voltage (V_g), normal resistance (R_N) and subgap resistance (R_L) were calculated from the measured dc I-V characteristics, see figure 1. The fitting parameter, a, which is associated with quasiparticle tunnel current onset sharpness in equation (11) was also estimated from the measured dc I-V characteristic. These parameters were implemented in equation (11) and (7) for $m = 0$ in order to extract the pumping factor, α, as illustrated in figure 6 for two different values.

The output power associated with the ac quasiparticle tunnel current was recorded for different bias voltages at $\alpha \approx 0.85$ and $\alpha \approx 3$ at an input source frequency of 93 GHz. Figure 7 shows the measured modulus of the induced current at $\alpha \approx 0.85$ whereas figure 8 show the output power with respect to bias voltage and $\alpha \approx 3$.

The pumping factor of $\alpha \approx 0.85$ was extracted by following the procedure described in section II D. The modelled and measured current modulus are in good correspondence for the extracted pumping factor taking into consideration that the modeling did not account for changes in the delivered to the junction pumping power vs DC bias. The peak values of the modeled and the measured current modulus at $V - \hbar\omega_{RF}/e$ are almost identical, see figure 7. Thus, the peak value

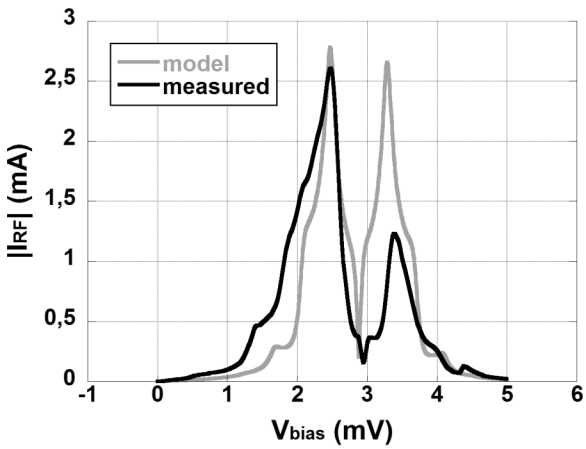

FIG. 7. The modulus of the induced QTC at pumping level $\boldsymbol{\alpha \approx 085}$. The QTC modulus is compared with the modelled QTC modulus where the loss of the junctions is not included.

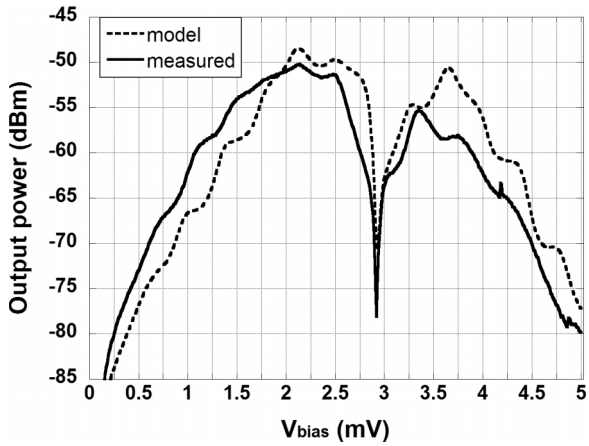

FIG. 8. A comparison of the measured and predicted power at the 2nd harmonic vs. bias voltage and pumping factor $\boldsymbol{\alpha \approx 3}$. The peak powers are due to the real part of current response function, i.e., I_{KK}. The figure shows excellent correspondence between model and measurement.

of the reactive QTC calculated using the modelled dc I-V characteristics and the Kramers-Kronig transform corresponds to the measured peak value of the reactive QTC.

Figure 8 compares the measured and predicted power of the second harmonic at $\alpha \approx 3$. The pumping factor was extracted in a similar manner as described in the section II D. Furthermore, it can be seen that all the fine structure of the theoretically predicted curve (equation (8)-(9)) could be found in the measured data. The fine structures in figure 8 are separated exactly by the voltage corresponding to the multiple of the applied rf photon size. Thereby, figure 8 clearly shows the presence of the multiphoton processes, as discussed in section II. There is a minor deviation close to the gap voltage between the model and the measurement data. Furthermore, the measured current envelop seems to be slightly wider than that of the model. These deviations could probably be attributed to three different effects. Firstly, as we suspect, the Josephson effect was not entirely suppressed, thus, allowing the very sensitive SIS down converter to detect the power due to the non-zero current in the vicinity of zero bias voltage. Secondly, the subgap current was slightly larger in reality than the estimated subgap current used in the model, which was based on dc measurements at liquid helium. The difference in the subgap current is probably due to a minor heating caused by the rf signal and a slight suppression of the superconductivity by the external magnetic field (for suppressing the Josephson effect). The third reason could be attributed to the possible limitations of measurement setup itself, e.g., stability of the rf source at 93 GHz. Nonetheless, the measured power of the second harmonic shown in Figure 8 is in good agreement with the theoretically predicted power and corresponds to the features predicted by the model attributed to the contribution from the I_{KK}. The experimental results and modeling allow us to consider applications of the SIS junction as a comb-generator or a multiplier to attain useful level of power at second harmonic as demonstrated here and possibly at higher order harmonics e.g., 3rd or 4th harmonic.

V. CONCLUSIONS

In this paper, it was shown both through theory and experiment that the reactive of the QTC of the SIS junction could be directly measured at specific bias voltages for the higher harmonics of the QTC. The measured reactive QTC at the specific bias voltage is in good agreement with theoretically calculated value at the same conditions. In order to measure the reactive current, the QTC harmonic behavior had to be studied both theoretically and experimentally. We used the theory of the quasiparticle tunneling to study the higher harmonics of the QTC in SIS junction in the presence of rf radiation. The impact of the reactive current on the harmonic behavior of the QTC was carefully studied by implementing a practical model with four parameters to model the dc I-V characteristics of the SIS junction. The reactive current was then calculated using the Kramers-Kronig

transform of the modelled dc I-V characteristics. The model has shown to be very useful due to its relative simplicity and ability to help getting deeper insight of the dc current response function (which corresponds to the dissipative and reactive current), and thus, the quasiparticle tunnel current at any harmonic of the input signal, since its completely defined by the dc I-V characteristics of the SIS junction and its Kramers-Kronig transform. This study shows that there is an excellent correspondence between the behavior of the predicted higher harmonic using previously established theory of the quasiparticle tunnel current in SIS junctions by J.R. Tucker and M.J. Feldman[5] and the measurements presented in this paper.

ACKNOWLEDGMENTS

We would like to thank Dr. Denis Meledin and T. Lic. Erik Sundin for their help with the arranging and testing of measurement equipment.

[1] B. D. Josephson, Physics Letters **1**(7), 251 (1962).
[2] B. D. Josephson, Reviews of Modern Physics **46**(2), 251 (1974).
[3] P. K. Tien and J. P. Gordon, Physical Review **129**(2), 647 (1963).
[4] N. R. Werthamer, Physical Review **147**(1), 255 (1966).
[5] John R. Tucker and Marc J. Feldman, Reviews of Modern Physics **57**(4), 1055 (1985).
[6] Qing Hu, C. A. Mears, P. L. Richards, and F. L. Lloyd, Physical Review Letters **64**(24), 2945 (1990).
[7] A. H. Worsham, N. G. Ugras, D. Winkler, D. E. Prober, N. R. Erickson, and P. F. Goldsmith, Physical Review Letters **67**(21), 3034 (1991).
[8] H. D. Foltz and J. H. Davis, presented at the Microwave Symposium Digest, 1990., IEEE MTT-S International, 1990 (unpublished).
[9] H. Rashid, V. Desmaris, A. Pavolotsky, and V. Belitsky, presented at the Infrared, Millimeter, and Terahertz waves (IRMMW-THz), 2014 39th International Conference on, 2014 (unpublished).
[10] B. Billade, A. Pavolotsky, and V. Belitsky, Terahertz Science and Technology, IEEE Transactions on **4**(2), 254 (2014).
[11] A. B. Ermakov, S. V. Shitov, A. M. Baryshev, V. P. Koshelets, and Willem Luinge, Applied Superconductivity, IEEE Transactions on **11**(1), 840 (2001).
[12] Alexey B. Pavolotsky, Dimitar Dochev, and Victor Belitsky, Journal of Applied Physics **109**(2), (2011).
[13] B. Billade, A. Pavolotsky, and V. Belitsky, Terahertz Science and Technology, IEEE Transactions on **3**(4), 416 (2013).